

## Electromagnetic Form Factors for the $\Lambda(1405)$

---

### **Benjamin J. Menadue\***

*Special Research Centre for the Subatomic Structure of Matter,  
School of Chemistry & Physics, University of Adelaide, SA 5005, Australia, and  
National Computational Infrastructure,  
Australian National University, Canberra, ACT 0200, Australia*  
E-mail: ben.menadue@adelaide.edu.au

### **Waseem Kamleh**

*Special Research Centre for the Subatomic Structure of Matter,  
School of Chemistry & Physics, University of Adelaide, SA 5005, Australia*  
E-mail: waseem.kamleh@adelaide.edu.au

### **Derek B. Leinweber**

*Special Research Centre for the Subatomic Structure of Matter,  
School of Chemistry & Physics, University of Adelaide, SA 5005, Australia*  
E-mail: derek.leinweber@adelaide.edu.au

### **M. Selim Mahbub**

*Special Research Centre for the Subatomic Structure of Matter,  
School of Chemistry & Physics, University of Adelaide, SA 5005, Australia, and  
CSIRO Computational Informatics, College Road, Sandy Bay, TAS 7005, Australia*  
E-mail: md.mahbub@adelaide.edu.au

### **Benjamin J. Owen**

*Special Research Centre for the Subatomic Structure of Matter,  
School of Chemistry & Physics, University of Adelaide, SA 5005, Australia*  
E-mail: benjamin.owen@adelaide.edu.au

Building on our successful technique to isolate the otherwise-elusive  $\Lambda(1405)$  using correlation matrix techniques and multiple source and sink smearings, we present calculations of the quark sector contributions to the electric form factors of the  $\Lambda(1405)$ . Using the PACS-CS (2 + 1)-flavour full-QCD ensembles available through the ILDG, our calculations reveal behaviour consistent with the development of a non-trivial molecular  $\bar{K}N$  bound-state component as one approaches the physical values of the  $u$  and  $d$  quark masses.

*31st International Symposium on Lattice Field Theory - LATTICE 2013  
July 29 - August 3, 2013  
Mainz, Germany*

---

\*Speaker.

## 1. Introduction

### 1.1 Motivation

The  $\Lambda(1405)$  is the lowest-lying odd-parity state of the  $\Lambda$  baryon. With a mass of  $1405.1^{+1.3}_{-1.0}$  MeV, it is lower than the lowest odd-parity state of the non-strange nucleon ( $N(1535)$ ). We now understand this unusually low mass to be a consequence of its flavour-singlet structure [1, 2, 3].

While early lattice QCD studies of this state were unable to reproduce the associated mass suppression, an extrapolation of the trend of the lowest-lying state in our recent work [4] was consistent with the physical mass of the  $\Lambda(1405)$ . The use of a correlation matrix is key to this success. Away from the  $SU(3)$ -flavour-symmetry limit, octet and singlet state components are strongly mixed. A correlation matrix analysis is required to isolate the QCD eigenstates and reveal the non-trivial mixing of octet and singlet components. Subsequent studies have confirmed our results [5].

Key to our work’s success is the inclusion of both multiple source and sink smearings, and multiple flavour and Dirac structures in the choice of interpolating fields. Figure 1 displays the flavour composition of the  $\Lambda(1405)$  in the relative components of the different interpolating fields from a  $6 \times 6$  correlation matrix as the pion-mass varies. While the highly-smeared, flavour-singlet operator is always the dominant contribution, an octet component becomes important away from the  $SU(3)$ -flavour-symmetry limit. It’s also interesting to observe the smaller role for the 16-sweep-smeared flavour-singlet interpolator as the  $u$  and  $d$  quark masses become light.

The variational analysis is also necessary to obtain a signal that is stable for sufficiently long Euclidean times after the fermion source (in our case,  $t = 16$ ) to perform the current insertion for the form factor analysis. Figure 2 demonstrates the long-term stability of the correlation function extracted from the variational analysis. We insert the current at  $t = 21$ , five time slices after the fermion source. Here the variational analysis provides optimal coupling to the lowest state and effective suppression of excited state contaminations. Moreover, the two-point correlation function

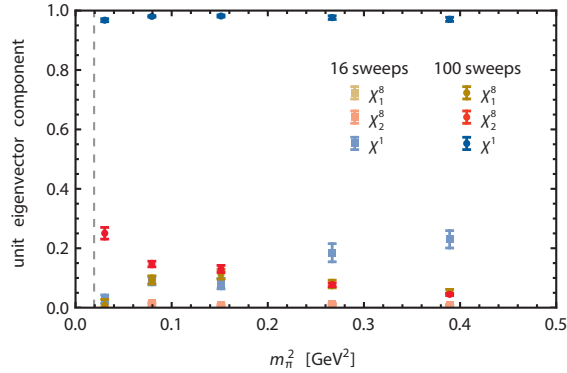


**Figure 1:** Relative strength of each interpolating field’s eigenvector component,  $u_i(\mathbf{0})$  of Eq. (2.4), for the  $\Lambda(1405)$  as a function of  $m_\pi^2$ . The light-coloured points are smeared with 16 sweeps of smearing and the dark points with 100 sweeps. The gold points correspond to the flavour-octet operator with a  $(qC\gamma_5 q)q$  Dirac structure, the red points correspond to the same flavour-octet structure but with a  $(qCq)\gamma_5 q$  Dirac structure. The blue points correspond to the flavour-singlet operator.

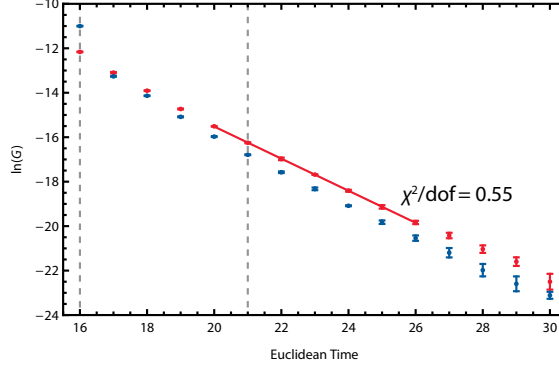


**Figure 2:** Comparison between the correlation functions extracted from a variational analysis (red) and from a traditional analysis (blue). The variational analysis results in a lower slope that is constant over a larger fit window, indicating a more complete isolation of the lowest-lying state. The fermion source is at  $t = 16$  (first dashed line), and the current insertion for the form factor analysis is at  $t = 21$  (second dashed line).

remains stable long enough after the current insertion to extract reasonable measures of the form factors.

## 1.2 Simulation Details

We use the PACS-CS  $(2+1)$ -flavour full-QCD ensembles [6], made available through the ILDG [7]. These ensembles have a lattice size of  $32^3 \times 64$  with  $\beta = 1.90$ , and there are five pion masses ranging from 640 MeV down to 156 MeV. Each ensemble has the same dynamical strange quark mass, corresponding to  $\kappa_s = 0.13640$ , however we perform our simulations using  $\kappa_s = 0.13665$  for the valence strange quarks to reproduce the correct kaon mass in the physical limit. As demonstrated in Ref. [1], this partial quenching is subtle and doesn't affect the extracted form factors. We consider setting the scale using both the Sommer and PACS-CS schemes, however we find no qualitative difference between them in the behaviour of the form factors. We select the PACS-CS scheme in the following.

## 2. Techniques

### 2.1 Two-Point Variational Analysis

To extract correlation functions from a variational analysis [8], we first need to construct the correlation matrix. If we consider some set of operators  $\{\chi_i\}$  that couple to the states of interest, the associated correlation matrix can be written as

$$G_{ij}(\Gamma; \mathbf{p}; t) = \sum_{\mathbf{x}} e^{-i\mathbf{p}\cdot\mathbf{x}} \text{tr}(\Gamma \langle \Omega | \chi_i(x) \bar{\chi}_j(0) | \Omega \rangle), \quad (2.1)$$

where  $\Gamma$  is some Dirac matrix that sensibly selects the appropriate components of the resultant spinor matrix. We then solve for the left ( $\mathbf{v}^\alpha(\mathbf{p})$ ) and right ( $\mathbf{u}^\alpha(\mathbf{p})$ ) generalised eigenvectors of  $G(\Gamma; \mathbf{p}; t + \delta t)$  and  $G(\Gamma; \mathbf{p}; t)$ , so that

$$G(\Gamma; \mathbf{p}; t + \delta t) \mathbf{u}^\alpha(\mathbf{p}) = e^{-E_\alpha(\mathbf{p})\delta t} G(\Gamma; \mathbf{p}; t) \mathbf{u}^\alpha(\mathbf{p}), \quad \text{and} \quad (2.2)$$

$$\mathbf{v}^{\alpha\top}(\mathbf{p}) G(\Gamma; \mathbf{p}; t + \delta t) = e^{-E_\alpha(\mathbf{p})\delta t} \mathbf{v}^{\alpha\top}(\mathbf{p}) G(\Gamma; \mathbf{p}; t). \quad (2.3)$$

These eigenvectors identify the “ideal” combinations  $\phi^\alpha$  of the original operators  $\chi_i$  that perfectly isolate individual energy eigenstates at momentum  $\mathbf{p}$ . As such, we can write

$$\phi^\alpha(\mathbf{p}) = v_i^\alpha(\mathbf{p}) \chi_i \quad \bar{\phi}^\alpha(\mathbf{p}) = \bar{\chi}_i u_i^\alpha(\mathbf{p}). \quad (2.4)$$

Note that the Greek indices,  $\alpha$  and  $\beta$ , label states and are not to be summed over; unlike the Latin operator indices ( $i, j, \dots$ ) which are summed over. Using these operators, we can extract correlation functions for the individual eigenstates,

$$G_\alpha(\Gamma; \mathbf{p}; t) = \sum_{\mathbf{x}} e^{-i\mathbf{p}\cdot\mathbf{x}} \text{tr}(\Gamma \langle \Omega | \phi^\alpha(x) \bar{\phi}^\alpha(0) | \Omega \rangle) \quad (2.5)$$

$$= \sum_{\mathbf{x}} e^{-i\mathbf{p}\cdot\mathbf{x}} \text{tr}(\Gamma \langle \Omega | v_i^\alpha(\mathbf{p}) \chi_i \bar{\chi}_j u_j^\alpha(\mathbf{p}) | \Omega \rangle) \quad (2.6)$$

$$= v_i^\alpha(\mathbf{p}) \left( \sum_{\mathbf{x}} e^{-i\mathbf{p}\cdot\mathbf{x}} \text{tr}(\Gamma \langle \Omega | \chi_i \bar{\chi}_j | \Omega \rangle) \right) u_j^\alpha(\mathbf{p}) \quad (2.7)$$

$$= \mathbf{v}^{\alpha\top}(\mathbf{p}) G(\Gamma; \mathbf{p}; t) \mathbf{u}^\alpha(\mathbf{p}). \quad (2.8)$$

## 2.2 Three-point Variational Analysis

To extract the form factors for an energy eigenstate  $\alpha$ , we need to calculate the three-point correlation function

$$G_\alpha^\mu(\Gamma; \mathbf{p}', \mathbf{p}; t_2, t_1) = \sum_{\mathbf{x}_1, \mathbf{x}_2} e^{-i\mathbf{p}'\cdot\mathbf{x}_2} e^{i(\mathbf{p}'-\mathbf{p})\cdot\mathbf{x}_1} \text{tr}(\Gamma \langle \Omega | \phi^\alpha(x_2) j^\mu(x_1) \bar{\phi}^\alpha(0) | \Omega \rangle). \quad (2.9)$$

where  $j^\mu$  is the current. This takes the form

$$G_\alpha^\mu(\Gamma; \mathbf{p}', \mathbf{p}; t_2, t_1) = e^{-E_\alpha(\mathbf{p}')(t_2-t_1)} e^{-E_\alpha(\mathbf{p})t_1} \text{tr} \left( \Gamma \sum_{s, s'} \langle \Omega | \phi^\alpha | p', s' \rangle \langle p', s' | j^\mu | p, s \rangle \langle p, s | \bar{\phi}^\alpha | \Omega \rangle \right) \quad (2.10)$$

where the current matrix element  $\langle p', s' | j^\mu | p, s \rangle$  encodes the form factors of the interaction.

Using the nature of the “perfect” operators  $\phi^\alpha$ , we can rewrite this perfect three-point correlation function in terms of the non-projected three-point correlation functions  $G_{ij}^\mu$  calculated using the original operators  $\chi_i$  using

$$G_\alpha^\mu(\Gamma; \mathbf{p}', \mathbf{p}; t_2, t_1) = \sum_{\mathbf{x}_1, \mathbf{x}_2} e^{-i\mathbf{p}'\cdot\mathbf{x}_2} e^{i(\mathbf{p}'-\mathbf{p})\cdot\mathbf{x}_1} \text{tr}(\Gamma \langle \Omega | v_i^\alpha(\mathbf{p}') \chi^i(x_2) j^\mu(x_1) \bar{\chi}_j(0) u_j^\alpha(\mathbf{p}) | \Omega \rangle) \quad (2.11)$$

$$= \mathbf{v}^{\alpha\top}(\mathbf{p}') G^\mu(\Gamma; \mathbf{p}', \mathbf{p}; t_2, t_1) \mathbf{u}^\alpha(\mathbf{p}). \quad (2.12)$$

To eliminate the temporal dependence of the three-point correlation function, we construct the ratio [9, 10]

$$R_\alpha^\mu(\Gamma', \Gamma; \mathbf{p}', \mathbf{p}; t_2, t_1) = \left( \frac{G_\alpha^\mu(\Gamma; \mathbf{p}', \mathbf{p}; t_2, t_1) G_\alpha^\mu(\Gamma'; \mathbf{p}', \mathbf{p}; t_2, t_1)}{G_\alpha(\Gamma'; \mathbf{p}'; t_2) G_\alpha(\Gamma; \mathbf{p}; t_2)} \right)^{1/2}, \quad (2.13)$$

and then to further simplify things define a reduced ratio as

$$\bar{R}_\alpha^\mu(\Gamma', \Gamma; \mathbf{p}', \mathbf{p}; t_2, t_1) = \left( \frac{2E_\alpha(\mathbf{p})}{E_\alpha(\mathbf{p}) + m_\alpha} \right)^{1/2} \left( \frac{2E_\alpha(\mathbf{p}')}{E_\alpha(\mathbf{p}') + m_\alpha} \right)^{1/2} R_\alpha^\mu(\Gamma', \Gamma; \mathbf{p}', \mathbf{p}; t_2, t_1) \quad (2.14)$$

### 2.3 Choice of Operators

Since the  $\Lambda$  baryon lies in the centre of the  $SU(3)$ -flavour symmetry group, there are many operators that will couple to it. We can consider interpolating fields having either a flavour-octet or -singlet symmetry structure, in addition to the usual two Dirac structures. (We note that the two Dirac structures are related through a Fierz transformation for the flavour-singlet operator.) These operators have the forms [9]

$$\chi_1^8 = \frac{1}{\sqrt{6}} \varepsilon^{abc} \left( 2(u^a C \gamma_5 d^b) s^c + (u^a C \gamma_5 s^b) d^c - (d^a C \gamma_5 s^b) u^c \right), \quad (2.15)$$

$$\chi_2^8 = \frac{1}{\sqrt{6}} \varepsilon^{abc} \left( 2(u^a C d^b) \gamma_5 s^c + (u^a C s^b) \gamma_5 d^c - (d^a C s^b) \gamma_5 u^c \right), \text{ and} \quad (2.16)$$

$$\chi^1 = 2\varepsilon^{abc} \left( (u^a C \gamma_5 d^b) s^c - (u^a C \gamma_5 s^b) d^c + (d^a C \gamma_5 s^b) u^c \right), \quad (2.17)$$

where we have suppressed the  $x$  dependence for clarity. We also expand our operator basis by including operators smeared by differing amounts of gauge-invariant Gaussian smearing [11].

Note that if too few operators are included, the states won't be sufficiently isolated, while if we include too many the correlation matrix will be too ill-conditioned to solve for the generalised eigenvectors. We focus on the  $6 \times 6$  matrix formed by using  $\chi_1^8$ ,  $\chi_2^8$ , and  $\chi^1$  together with 16 and 100 sweeps of smearing. The selection of these two smearings gives results consistent with other smearing combinations involving at least one of 100 or 200 smearing sweeps, but offer reduced statistical noise.

### 2.4 Extracting Form Factors

Once we have calculated the reduced ratio  $\bar{R}_\alpha^\mu$  for some energy eigenstate  $\alpha$ , we can turn our attention to extracting information such as the form factors of the interaction. The current matrix element for spin-1/2 baryons can be written in the form

$$\langle p', s' | j^\mu | p, s \rangle = \left( \frac{m_\alpha^2}{E_\alpha(\mathbf{p}) E_\alpha(\mathbf{p}')} \right)^{1/2} \bar{u} \left( F_1(q^2) \gamma^\mu + i F_2(q^2) \sigma^{\mu\nu} \frac{q^\nu}{2m_\alpha} \right) u, \quad (2.18)$$

where  $F_1$  and  $F_2$  are the Dirac and Pauli form factors. These are related to the Sachs form factors through

$$\mathcal{G}_E(q^2) = F_1(q^2) - \frac{q^2}{(2m_\alpha)^2} F_2(q^2), \text{ and} \quad (2.19)$$

$$\mathcal{G}_M(q^2) = F_1(q^2) + F_2(q^2). \quad (2.20)$$

A suitable choice of momentum  $\mathbf{q}$  and the Dirac matrices  $\Gamma$  and  $\Gamma'$  allows us to directly access the Sachs form factors through an ‘‘effective’’ form factor [9]. In particular, we have

$$\mathcal{G}_E^{\text{eff},\alpha}(q^2) = \bar{R}_\alpha^\mu(\Gamma_4^\pm, \Gamma_4^\pm; \mathbf{q}, \mathbf{0}; t_2, t_1), \text{ and} \quad (2.21)$$

$$|\varepsilon_{ijk} q^i| \mathcal{G}_M^{\text{eff},\alpha}(q^2) = (E_\alpha(\mathbf{q}) + m_\alpha) \bar{R}_\alpha^\mu(\Gamma_j^\pm, \Gamma_4^\pm; \mathbf{q}, \mathbf{0}; t_2, t_1), \quad (2.22)$$

where the appropriate Dirac matrices are

$$\Gamma_j^+ = \frac{1}{2} \begin{bmatrix} \sigma_j & 0 \\ 0 & 0 \end{bmatrix}, \quad \Gamma_4^+ = \frac{1}{2} \begin{bmatrix} \mathbb{I} & 0 \\ 0 & 0 \end{bmatrix}, \quad (2.23)$$

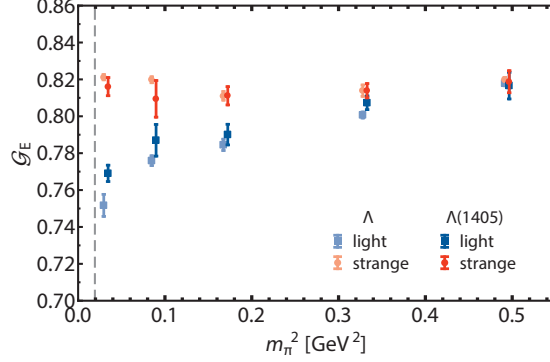


**Figure 3:** Sachs electric form factors at  $Q^2 = 0.16 \text{ GeV}^2/c^2$ . Results for the individual unit-charged quark flavour sectors for the  $\Lambda(1405)$  (dark points) are compared with those for the ground state  $\Lambda$  (light).

for the positive-parity states and

$$\Gamma_j^- = -\gamma_5 \Gamma_j^+ \gamma_5 = \frac{1}{2} \begin{bmatrix} 0 & 0 \\ 0 & \sigma_j \end{bmatrix}, \quad \Gamma_4^- = -\gamma_5 \Gamma_4^+ \gamma_5 = \frac{1}{2} \begin{bmatrix} 0 & 0 \\ 0 & \mathbb{I} \end{bmatrix}, \quad (2.24)$$

for negative parity.

Since the momentum transfer for a constant current momentum depends on the mass of the target, to obtain accurate comparisons we need to correct for any subtle changes in  $Q^2$ . To do this, we assume that  $\mathcal{G}_E$  has a dipole dependence on  $Q^2$ , so that

$$\mathcal{G}_E(Q^2) = \left( \frac{\Lambda}{\Lambda + Q^2} \right)^2 \mathcal{G}_E(0). \quad (2.25)$$

We can solve for  $\Lambda$  by taking our measured  $\mathcal{G}_E(Q^2)$  in combination with the  $\mathcal{G}_E(0) = 1$  implication of the unit-charge normalisation. This can then be used to evaluate  $\mathcal{G}_E$  at any nearby  $Q^2$ . Since there is little variation in  $Q^2$  across the range of  $m_\pi^2$  under consideration, this is a small correction.

### 3. Results

Figure 3 presents the pion mass dependence of the Sachs electric form factors for the individual quark sectors for both the  $\Lambda(1405)$  and the ground-state even-parity  $\Lambda$  at  $Q^2 = 0.16 \text{ GeV}^2/c^2$ . We see little change between the ground state  $\Lambda$  and the  $\Lambda(1405)$ . At heavy quark masses approaching the flavour-symmetry limit, the light ( $u$  or  $d$ ) quarks in the  $\Lambda(1405)$  have the same distribution as the strange quark as required by the singlet symmetry. As the  $u$  and  $d$  quarks become light, we observe a significant departure from the flavour symmetry, reminiscent of Fig. 1 where the octet interpolator becomes important for the excitation of the  $\Lambda(1405)$  in the light-quark region. It is also interesting to note that the strange quark form factor variation is a pure environment effect as the mass of the strange quark is held fixed.

The deviation from this flavour-singlet picture as the pion mass approaches its physical value is consistent with the development of a  $\bar{K}N$  component in the structure of the  $\Lambda(1405)$ . If we consider such a dressing, the centre of mass lies nearer the heavier nucleon, so the anti-light-quark contribution is distributed further out by the  $\bar{K}$ ; this leaves an enhanced light-quark form factor.

Similarly, the strange quark is also distributed further out by the  $\bar{K}$  and thus results in a suppressed form factor relative to the ground state  $\Lambda$ .

#### 4. Conclusion

Variational techniques provide a robust technique for accessing and isolating the eigenstates of QCD on a finite volume lattice. In the case of the  $\Lambda(1405)$  the correlation matrix is vital in separating the nearby octet and singlet states of the spectrum. Herein, we have presented the very first calculation of the electric form factors of the unusual  $\Lambda(1405)$ . Our results are consistent with the development of a non-trivial  $\bar{K}N$  bound-state component as one approaches the physical values of the  $u$  and  $d$  quark masses.

#### Acknowledgements

This research was undertaken with the assistance of resources at the NCI National Facility in Canberra, Australia, and the iVEC facilities at Murdoch University (iVEC@Murdoch) and the University of Western Australia (iVEC@UWA). These resources were provided through the National Computational Merit Allocation Scheme, supported by the Australian Government, and the University of Adelaide Partner Share. This research is supported by the Australian Research Council.

#### References

- [1] B. J. Menadue, W. Kamleh, D. B. Leinweber, M. S. Mahbub and B. J. Owen, *Electromagnetic form factors of the  $\Lambda(1405)$  in  $(2+1)$ -flavour lattice QCD*, PoS **LATTICE2012** (2012) 178.
- [2] B. J. Menadue, W. Kamleh, D. B. Leinweber and M. S. Mahbub, *The 1405-MeV Lambda resonance in full-QCD*, PoS **LATTICE2011** (2011) 129.
- [3] B. J. Menadue, W. Kamleh, D. B. Leinweber and M. S. Mahbub, *The Lambda(1405) in full QCD*, AIP Conf. Proc. **1418** (2011) 130.
- [4] B. J. Menadue, W. Kamleh, D. B. Leinweber and M. S. Mahbub, *Isolating the  $\Lambda(1405)$  in Lattice QCD*, Phys. Rev. Lett. **108** (2012) 112001 [arXiv:1109.6716 [hep-lat]].
- [5] G. P. Engel, C. B. Lang and A. Schafer, *Low-lying  $\Lambda$  Baryons from the Lattice*, Phys. Rev. D **87** (2013) 3, 034502 [arXiv:1212.2032 [hep-lat]].
- [6] S. Aoki *et al.* [PACS-CS Collaboration], *2 + 1 Flavor Lattice QCD toward the Physical Point*, Phys. Rev. D **79** (2009) 034503 [arXiv:0807.1661 [hep-lat]].
- [7] M. G. Beckett, *et al.*, *Building the International Lattice Data Grid*, Comput. Phys. Commun. **182** (2011) 1208 [arXiv:0910.1692 [hep-lat]].
- [8] D. B. Leinweber, W. Melnitchouk, D. G. Richards, A. G. Williams and J. M. Zanotti, *Baryon spectroscopy in lattice QCD*, Lect. Notes Phys. **663** (2005) 71 [nucl-th/0406032].
- [9] D. B. Leinweber, R. M. Woloshyn and T. Draper, *Electromagnetic structure of octet baryons*, Phys. Rev. D **43** (1991) 1659.
- [10] S. Boinepalli, *et al.*, *Precision electromagnetic structure of octet baryons in the chiral regime*, Phys. Rev. D **74** (2006) 093005 [hep-lat/0604022].
- [11] S. Gusken, *A Study of smearing techniques for hadron correlation functions*, Nucl. Phys. Proc. Suppl. **17** (1990) 361.